Increased amyloidogenic secretion in cerebellar granule cells undergoing apoptosis

(Alzheimer disease/potassium deprivation/β amyloid)

Cinzia Galli*†, Alessandra Piccini*‡, Maria Teresa Ciotti*, Loriana Castellani§, Pietro Calissano*, Damiano Zaccheo‡, and Massimo Tabaton‡¶

*Istituto di Neurobiologia, Consiglio Nazionale delle Ricerche, Via K. Marx 43, 00137 Rome, Italy; ‡Istituto di Anatomia Umana and ¶Dipartimento di Neuroscienze, Università di Genova, Via De Toni 10, 16132 Genova, Italy; §Dipartimento di Medicina Sperimentale e di Scienze Biochimiche, Università di Roma Tor Vergata, Via di Tor Vergata 135, 00133 Rome, Italy

ABSTRACT Some clues suggest that neuronal damage induces a secondary change of amyloid β protein (Aβ) metabolism. We investigated this possibility by analyzing the secretion of Aβ and processing of its precursor protein (amyloid precursor protein, APP) in an *in vitro* model of neuronal apoptosis. Primary cultures of rat cerebellar granule neurons were metabolically labeled with [^{35}S]methionine. Apoptosis was induced by shifting extracellular KCl concentration from 25 mM to 5 mM for 6 h. Control and apoptotic neurons were then subjected to depolarization-stimulated secretion. Constitutive and stimulated secretion media and cell lysates were immunoprecipitated with antibodies recognizing regions of Aβ, full-length APP, α- and β-APP secreted forms. Immunoprecipitated proteins were separated by SDS/PAGE and quantitated with a PhosphorImager densitometer. Although intracellular full-length APP was not significantly changed after apoptosis, the monomeric and oligomeric forms of 4-kDa Aβ were 3-fold higher in depolarization-stimulated secretion compared with control neurons. Such increments were paralleled by a corresponding increase of the β-APP$_s$/α-APP$_s$ ratio in apoptotic secretion. Immunofluorescence studies performed with an antibody recognizing an epitope located in the Aβ sequence showed that the Aβ signal observed in the cytoplasm and in the Golgi apparatus of control neurons is uniformly redistributed in the condensed cytoplasm of apoptotic cells. These studies indicate that neuronal apoptosis is associated with a significant increase of metabolic products derived from β-secretase cleavage and suggest that an overproduction of Aβ may be the consequence of neuronal damage from various causes.

The main pathological features of Alzheimer disease (AD) are extracellular deposits of amyloid β protein (Aβ), intraneuronal abnormal cytoskeletal filaments, and synaptic loss. The "cascade" hypothesis suggests cerebral formation of amyloid fibers as the first event of AD pathogenesis and, thereby, increased accumulation of soluble forms of Aβ as the primary culprit of the disease. This hypothesis is supported by the following evidence (1): (*i*) the progression of cerebral lesions in Down's syndrome, in which soluble Aβ begins to accumulate in brain tissue at least three decades before the appearance of cytoskeletal changes; (*ii*) all known genetic alterations linked to familial AD lead to an increased production of different forms of soluble Aβ; and (*iii*) polymers of Aβ show cytotoxic effects *in vitro* and induce apoptosis in neuronal cultures. However, there are other clues arguing against the primary and unique role of cerebral Aβ accumulation in AD pathogenesis. Indeed,

quantitative pathological studies performed either in human brain or in transgenic mice expressing mutant amyloid precursor protein (APP) showed that the relationships among the extent of Aβ deposits, neuronal loss, and behavioral deficit are not constant (2), suggesting that a common phenotype, sharing the presence of various amounts of Aβ plaques, neurofibrillary tangles, and neuronal loss, may be the final effect of different primary etiologies. This point of view is supported by the recent finding that mutations of a gene linked to familial AD, presenilin 2 (PS2), causes apoptosis when expressed in PC12 cells (3). Because it has been reported that AD patients carrying this gene mutation present a classical pathological picture including an increase of the Aβ longer form (Aβ_{42}) in cerebrum and plasma (4), it is reasonable to speculate that apoptosis caused by a PS2 mutation is followed and not preceded by increased Aβ production. Furthermore, it is possible to speculate that the cellular damage leading to neuronal apoptosis caused by a different primary cause induces an overproduction of Aβ and that this event occurs in the pathogenesis of AD, in which apoptotic neurons have been shown to be present in the affected brain regions (5).

We investigated this issue by analyzing the changes of Aβ metabolism after apoptosis induced in cerebellar granule cells by KCl deprivation. This model of neuronal apoptosis bears methodological advantages as described (6, 7) and represents the *in vitro* counterpart of neuronal deafferentation. Moreover, the removal of depolarizing stimuli obtained by lowering extracellular KCl from 25 mM to 5 mM changes most of the voltage-dependent events such as channels opening, intracellular Ca^{2+} signaling (8, 9), neurotransmitters (10), and neuropeptides secretion (11). Herein we report that this model of neuronal apoptosis is accompanied by a 3-fold increase of total Aβ secretion, in spite of the presence of a normal production of APP. These findings and the observed changes of the other secreted APP derivatives (APP$_s$) indicate that neuronal apoptosis induces changes in APP intracellular trafficking and cleavage that are indicative of a preferential amyloidogenic metabolism occurring in cerebellar granule cells undergoing apoptosis.

MATERIALS AND METHODS

Neuronal Cultures. Primary cultures of cerebellar granule neurons were obtained from dissociated cerebella of 8-day-old Wistar rats (Charles River Breeding Laboratories) (12). Cells were plated in basal medium Eagle (BME; GIBCO/BRL) supplemented with 10% fetal calf serum, 25 mM KCl, 2 mM

---

glutamine (GIBCO/BRL), and gentamicin (GIBCO/BRL; 100 μg/ml) on poly-(L-lysine)-coated dishes (Nunc). At plating, cell density was 3×10^5 per cm^2 (15×10^6 cells per 100-mm dish). Cytosine β-D-arabinofuranoside (10 μM) was added to the culture medium 18–22 h after plating to prevent proliferation of nonneuronal cells.

Metabolic Labeling and Apoptosis Induction. After 6 days *in vitro*, cerebellar granule cells were metabolically labeled by an overnight incubation in methionine-free DMEM containing 2 mM glutamine, 25 mM KCl, and [^{35}S]methionine (80 μCi/ml; 1 Ci = 37 GBq). Labeled neurons were subsequently treated for apoptosis induction by two washes with BME containing 5 mM KCl (5 mM KCl/BME) and incubated in 5 ml of the same medium. Control cells were incubated in the same medium supplemented with 25 mM KCl. After 6 h of incubation, the medium containing constitutive secretion (CS) products was collected. Control and apoptotic neurons were both preincubated in 5 mM KCl/BME for 15 min and subsequently subjected to a release experiment as described (10, 11, 13) with minor modifications. Briefly, neurons were subjected to a depolarizing secretory stimulus by 30 min of incubation in 5 ml of high KCl Locke solution (98 mM NaCl/56 mM KCl/2.3 mM CaCl$_2$/0.4 mM MgCl$_2$/5.6 mM glucose/10 mM Hepes, pH 7.4). This treatment causes release from secretory vesicles of neurotransmitters and neuropeptides (10, 11, 13). After incubation, the solution containing depolarization stimulated secretion (DSS) products was collected. Neurons were lysed in 1 ml of RIPA lysis buffer (14).

Immunoprecipitation and Gel Electrophoresis. Cell lysates and secretion media (CS and DSS) supplemented with protease inhibitors [leupeptin (1 μg/ml)/pepstatin (0.1 μg/ml)/2 mM phenylmethylsulfonyl fluoride) were processed for detection of Aβ, APP, and APP$_s$. The following antibodies, directed against the epitopes reported in Fig. 1, were used: polyclonal antibody R3659, raised against Aβ synthetic peptide containing residues 1–40 (15) and recognizing residues 1–5 of Aβ (16); monoclonal antibody 6E10, specific for Aβ residues 1–17 (17) and immunoreactive with α- but not β-APP$_s$; mAb 22C11 (Boeheringer Mannhein) recognizing N-terminal portion of APP (residues 60–100); polyclonal antibody C7, raised to synthetic APP residues 732–751 (18); polyclonal antibodies R1872 and R1155, recognizing APP epitopes flanking the Aβ portion (R1872 residues 652–671 and R1155 residues 714–730) (19). Immunoprecipitation of cell lysates and CS and DSS media was performed overnight at 4°C with the corresponding antibody preadsorbed for 2 h at 4°C with protein A-agarose. After immunoprecipitation, samples were centrifuged at 3,000 rpm in an Eppendorf centrifuge and pellets were washed seven times with PBS. For detection of Aβ, samples were resuspended in 30 μl of 2× sample buffer (8% SDS/24% glycerol/100 mM Tris/100 mM Tricine/Coomassie blue G250), boiled for 5 min, and subsequently analyzed by Tris-Tricine SDS/PAGE on 10–18% gels. For detection of APP and APP$_s$, immunoprecipitated samples were resuspended in 20 μl of 2× sample buffer (9 M urea/75 mM Tris·HCl/140 mM 2-mercaptoethanol/2% SDS), boiled, and separated on 10% and 7.5% SDS/PAGE gels, respectively. Radiolabeled bands were quantitated with a PhosphorImager densitometer (Molecular

Dynamics) using IMAGE QUANT software. The gels were also analyzed by routine autoradiographic methods.

Immunofluorescence Labeling. Neurons were grown 6–7 days *in vitro* on poly-(L-lysine)-coated glass coverslips, then rinsed three times with PBS, and fixed for 10 min with 4% (wt/vol) paraformaldehyde (in PBS). Cells were permeabilized for 5 min with 0.2% Triton X-100 in 100 mM Tris·HCl (pH 7.5). Incubation with mAb 4G8 (1:100 dilution; Seneteck, Maryland, MO) recognizing the region of Aβ residues 17–24 was carried out at room temperature and fluorescein isothiocyanate-conjugated goat anti-mouse IgG was used for detection. For Golgi apparatus labeling, cells were incubated for 30 min with rhodamine-conjugated wheat germ agglutinin (WGA; 1:200 dilution). For nuclear staining, cells were incubated with propidium iodide (0.2 μg/ml) for 5 min before being mounted in Gelvatol.

The samples were routinely examined with a Leitz Dialux 22 microscope, equipped with a ×50 water-immersion objective. Confocal analysis was carried out with a Leica TCS 4D system, equipped with a ×100 1.3–0.6 oil-immersion objective.

All chemicals were from Sigma.

RESULTS

Apoptosis was induced in cerebellar granule cells metabolically labeled with [^{35}S]methionine by lowering extracellular KCl concentration from 25 to 5 mM. After 6 h, conditioned medium from control and apoptotic neurons was collected and cells were subjected to a 30-min incubation in highly depolarizing KCl (56 mM), which causes release from secretory vesicles of neurotransmitters and neuropeptides (10, 11, 13).

The time of 6 hours after the beginning of the apoptotic stimulus was chosen because, as reported (6, 8), most of the neurons were still alive and morphologically well preserved but programmed cell death was irreversibly triggered in about 50% of neurons.

Secreted Aβ. Six hours after apoptotic stimulation, CS and DSS media were immunoprecipitated with R3659, the immunoprecipitate was separated by electrophoresis, and radioactivity in the gel was measured by PhosphorImaging (Fig. 2*A*). In CS medium of control and apoptotic neurons, no band was detected at 4 kDa, the predicted molecular weight of monomeric Aβ; a very weak signal (not reproducible by photography) was detected at 8 kDa; and a sharp band was visible at 14 kDa (Fig. 2*A*, lanes 1 and 2). Further, the immunoprecipitate from apoptotic neurons contained 2-fold more of the 8- and 14-kDa peptides compared with the immunoprecipitate from controls. In DSS medium of apoptotic neurons, in addition to the 8-kDa and 14-kDa bands, the 4-kDa monomeric Aβ was present (Fig. 2*A*, lane 3). In DSS medium from control neurons, the 14-kDa band was visible, whereas the 4- and 8-kDa bands were detectable only as PhosphorImager values. Preabsorption of R3659 with the synthetic Aβ peptide containing residues 1–40 abolished the immunoprecipitation of all three bands (Fig. 2*A*, lane 5). Phosphorimaging quantification showed a 3- and a 2.7-fold increase of 4-kDa and 14-kDa bands, respectively, in apoptotic DSS medium compared with control medium (Fig. 2*B*). To determine whether the 14-kDa band represents an Aβ oligomer or a fragment of APP containing the Aβ region, we first immunoprecipitated the DSS medium with antibodies recognizing APP epitopes flanking the N and C terminus of Aβ. The same medium was then incubated with R3659, and the 14-kDa band was still observed (Fig. 2*C*), suggesting that it represents trimers of Aβ. The 8-kDa band was not found in the analysis of the second immunoprecipitate, suggesting that it was bound by one of the antibodies flanking Aβ (Fig. 2*C*). Because the 8-kDa peptide was immunoprecipitated by R3659, which recognizes the N terminus of Aβ, and increased during the apoptotic process, we speculate that this
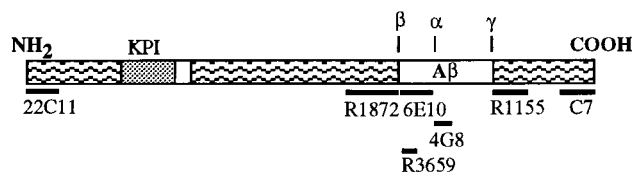
FIG. 1. Diagram showing the position of the APP$_{695}$ epitopes recognized by the various antibodies used in this study.
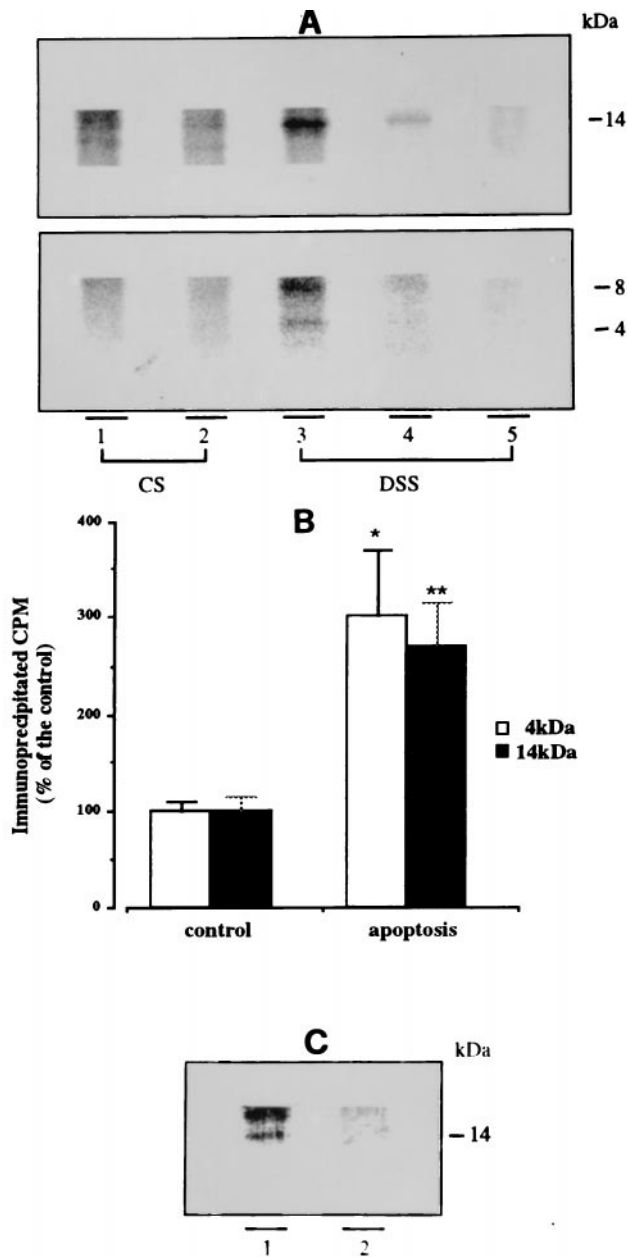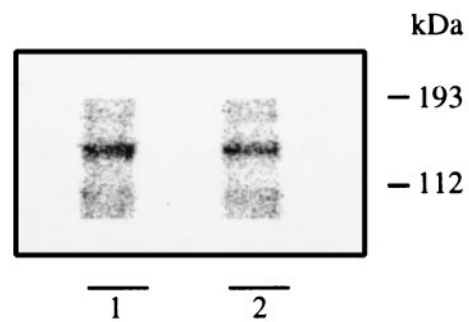
FIG. 3. Full-length APP is not increased in apoptotic neurons. Cells were labeled and apoptosis was triggered as described in Fig. 2. Cells were lysed and total proteins were immunoprecipitated with the C7 antibody and electrophoresed on 10% gels in glycine. Notice that full-length APP (130 kDa) is equal in control neurons (lane 2) and apoptotic cells (lane 1).

peptide corresponds to an APP C-terminal fragment containing the entire Aβ portion.

A consistently equal amount of total radioactivity was present in conditioned medium from control and apoptotic neurons in several experiments, thus, indicating that an equal amount of labeled proteins was released in control and experimental conditions. Therefore, the increase of Aβ forms was not the result of unspecific release of intracellular proteins caused by cell degeneration.

Full-Length Intracellular APP. The increase of the Aβ in CS and DSS media of apoptotic neurons could be the result of an increased amount of APP available for β-secretase cleavage. To test this hypothesis, immunoprecipitation of cell lysate with C7 was performed. The precipitates, analyzed by electrophoresis, revealed the presence of a 130-kDa peptide corresponding to the mature form of full-length APP (Fig. 3). When the full-length APP signal in control and apoptotic neurons was measured, no significant difference was found. Identical results were obtained when APP from whole-cell lysates was analyzed by Western blot (data not shown). To rule out the possibility that the 130-kDa peptide precipitated by C7 antibody was the APP-like protein 2, which has an electrophoretic mobility similar to APP (20) but lacks the Aβ portion (21, 22), an analogous immunoprecipitation of cell lysates was repeated with 6E10 antibody, which specifically recognizes APP. This antibody also immunoprecipitated the same 130-kDa peptide that was unchanged in controls and in apoptotic neurons (data not shown).

Secreted APP Derivatives. APP derivatives, resulting from α- and β-secretase cleavage (α- and β-APP$_s$), were extracted from cell-conditioned medium by two consecutive immunoprecipitations, first with the mAb 6E10, specific for the region of α-APP$_s$ corresponding to residues 1–17 of the Aβ sequence and second with the mAb 22C11, recognizing the N-terminal portion of APP, to immunoprecipitate β-APP$_s$. The first procedure resulted in a peptide of 100 kDa (α-APP$_s$), and the second immunoprecipitation yielded a band with a similar molecular mass (Fig. 4A), as expected for β-APP$_s$. We cannot exclude the possibility that part of the 100-kDa band obtained by the second immunoprecipitation with 22C11 originates from APP-like protein 2, which has a secreted N-terminal metabolite with a molecular mass similar to that of APP$_s$ (23). In control neurons, the amount of α-APP$_s$ (Fig. 4A, lane 2) was constantly higher than that of β-APP$_s$ (Fig. 4A, lane 4) in CS and in DSS media, confirming that physiological metabolism and secretion leads preferentially to the nonamyloidogenic

FIG. 2. Increased Aβ secretion in apoptotic neurons. After 7 days *in vitro*, cerebellar granule cells, metabolically prelabeled with [^{35}S]methionine, were incubated for 6 h in 25 mM KCl/BME (controls) or 5 mM KCl/BME (apoptosis) to obtain CS medium. Both apoptotic and control neurons were subsequently incubated 30 min in 56 mM KCl Locke solution to obtain DSS medium. CS and DSS media were subjected to immunoprecipitation and the immunoprecipitates were separated on Tris-Tricine 10–18% gels. (*A*) Electrophoretic analysis of R3659-immunoprecipitated proteins. Lanes: 1, 3, and 5, from apoptotic neurons; 2 and 4, controls. Monomeric (4 kDa) and putative Aβ oligomers (8 kDa and 14 kDa) are visible only in DSS medium from apoptotic neurons (lane 3), whereas the same three bands are barely detectable in control DSS medium (lane 4). The 14-kDa oligomeric Aβ is also detectable in apoptotic CS medium. Preabsorption of the antibody with synthetic Aβ (lane 5) abolished the appearance of both mono- and oligomeric forms. (*B*) PhosphorImaging quantification of 4-kDa (open bars) and 14-kDa (solid bars) bands obtained from DSS medium, shown in *A*, lanes 3 and 4. Values relative to apoptotic neurons are expressed as percent of controls. Both 4-kDa and 14-kDa bands originating from apoptotic DSS contain three times the amount of radioactivity compared with controls. ∗, $P < 0.002$ ($n = 4$); ∗∗, $P < 0.001$ ($n = 4$). (*C*) Apoptotic (lane 1) and control (lane 2) DSS media were immunoprecipitated simultaneously with Aβ "flanking" antisera R1155 and R1872 (see text). The supernatant was further incubated

with R3659 and the immunoprecipitated was analyzed by electrophoresis. Notice that the 14-kDa band is still present, but the 8-kDa peptide, probably isolated by one of the flanking antisera, is not visible.
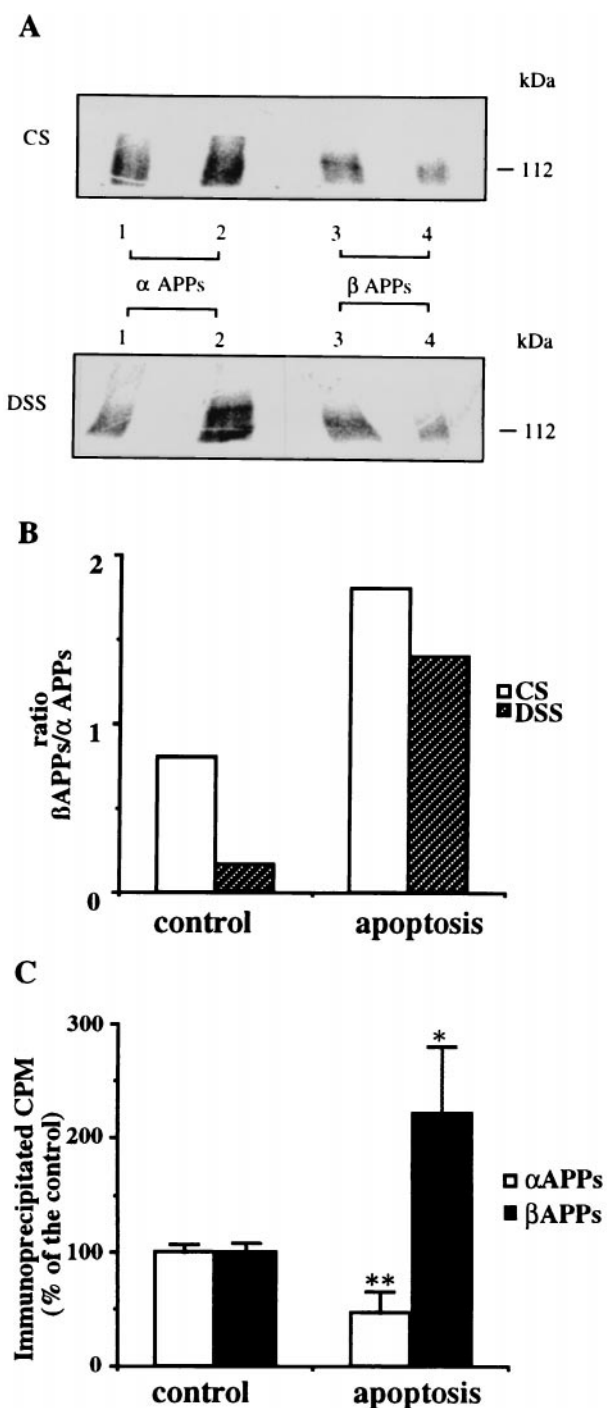
FIG. 4. Increase of β-APP$_s$ and decrease of α-APP$_s$ in apoptotic secretion. Cells were labeled and apoptosis was triggered as described in Fig. 2. (*A*) CS (*Upper*) and DSS (*Lower*) media from control (lanes 2 and 4) and apoptotic (lanes 1 and 3) neurons were collected and precipitated first with 6E10 (lanes 1 and 2) and reimmunoprecipitated with 22C11 (lanes 3 and 4). α-APP$_s$ (100 kDa), isolated with 6E10, is augmented in control secretions (both CS and DSS) with respect to apoptotic secretions. Conversely, β-APP$_s$ ($\sim$100 kDa), revealed by the second immunoprecipitation (see text), is increased in apoptotic secretions compared with controls. (*B*) Phosphorimaging quantification of the experiment shown in *A*. Histograms show the increase of the β-APP$_s$/α-APP$_s$ ratio in both CS (open bars) and DSS (solid bars) media. (*C*) Phosphorimaging of DSS medium as described in *A*. Histograms show the α-APP$_s$ decrease and the increase of β-APP$_s$ in DSS medium from apoptotic neurons compared with control neurons. *, $P < 0.02$; **, $P < 0.01$ ($n = 3$).

route (24, 25). Conversely, in apoptotic medium, β-APP$_s$ (Fig. 4*A*, lane3) levels were higher than α-APP$_s$ levels (Fig. 4*A*, lane 1), either in constitutive and stimulated secretion (for quantification, see also Fig. 4 *B* and *C*). Consequently, apoptosis produced a reversal of β-APP$_s$/α-APP$_s$ ratio, from 0.8 to 1.8 in CS (Fig. 4*B*, open bars) and from 0.2 to 1.4 in stimulated secretion (Fig. 4*B*, solid bars). In DSS medium, there was a 50% decrease of α-APP$_s$ and a 122% increase of β-APP$_s$ in apoptotic neurons compared with corresponding controls (Fig. 4*C*).

Immunofluorescence. Labeling of control neurons for Aβ protein showed a diffuse cytoplasmic distribution (Fig. 5*A*). An intense polarized signal caused by Aβ protein (Fig. 5*C*) was also observed at the level of the Golgi apparatus, identified by colocalization with WGA staining (Fig. 5 *D* and *E*). In apoptotic neurons, recognizable as cells with a small compacted nucleus strongly stained by propidium iodide (Fig. 5*B*, arrow), the Aβ reactivity remained condensed in cytoplasm (Fig. 5 *B* and *F*), whereas the Golgi apparatus became fragmented, as documented by weakening and dispersal of the WGA staining (Fig. 5*G*). This result is in agreement with a previous report describing fragmentation of the Golgi apparatus in apoptotic neurons (26). Therefore, in control neurons, Aβ immunoreactivity is mostly concentrated at the level of Golgi apparatus (Fig. 5*E*), whereas in apoptotic neurons the signal is redistributed through the condensed cytoplasm (Fig. 5*H*), suggesting a change of fate in the Aβ peptide trafficking. It is interesting to note that the change of Aβ signal distribution precedes the chromatin condensation, as seen in some preapoptotic neurons (Fig. 5*B*). These results and biochemical data documenting an increase in β-secretase products suggest that early accumulation of these species in a secretory compartment may occur.

DISCUSSION

Herein we show, in a *in vitro* model, that neuronal degeneration leading to apoptosis is accompanied by a significant increase of amyloidogenic metabolism of APP, characterized by oversecretion of total Aβ and β-APP$_s$ and a parallel decrease of α-APP$_s$ in absence of changes in full-length APP production. These findings result from the analysis of both CS and DSS, which are qualitatively coherent, although data obtained from DSS are quantitatively more clear. The length of time chosen for harvesting CS medium allows Aβ proteolysis by extracellular proteases (27) and may account, at least in part, for the discrepancy between CS and DSS. Interestingly, the apoptotic process is accompanied by increased formation of soluble Aβ aggregates in the secretion medium. The oligomerization of soluble Aβ occurs in cell medium at picomolar concentrations (19) and has been shown to increase in cells transfected with mutant PS genes, because of the higher proportion of the long A$\beta_{42(43)}$ (28). Although we were not able to quantify the percentages of Aβ_{40} and Aβ_{42}, because specific antibodies were not available, we speculate that the quick Aβ polymerization reflects a high level of Aβ_{42} in apoptotic secretion. A significant finding of our study is the elevated secretion of Aβ observed in cerebellar granule cells upon depolarizing stimulus, known to release neurotransmitters and neuropeptides from secretory vesicles (10, 11, 13). This result suggests the physiological presence of Aβ molecules in the secretory compartment in spite of the apparent undetectability of soluble intracellular Aβ. It is tempting to speculate that Aβ formation occurs concomitantly or just before the fusion of secretory vesicles with plasma membrane. Interestingly, DSS medium from apoptotic neurons contains a 3-fold higher amount of the monomeric Aβ compared with DSS medium from control neurons, suggesting that during the apoptotic process intracellular accumulation of APP metabolites, caused by a protein sorting derangement, leads to in-
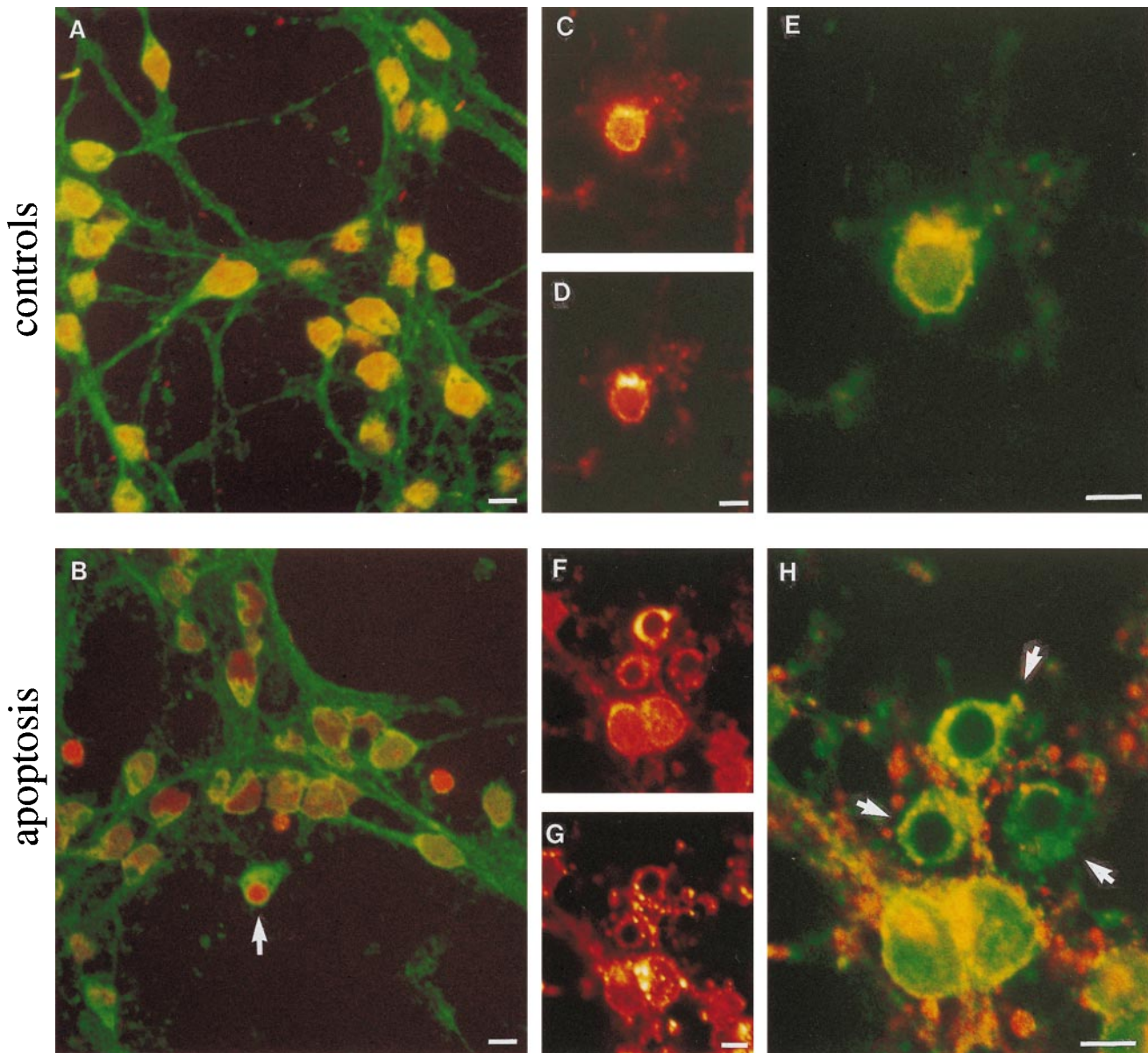
Fɪɢ. 5.   Cytoplasmic condensation of Aβ epitope and fragmentation of Golgi apparatus in cerebellar granule cells undergoing apoptosis. Confocal micrographs of controls (*A, C, D,* and *E*) and 6-h apoptotic (*B, F, G,* and *H*) neurons are shown. (*A* and *B*) Neurons were double-labeled with 4G8 antibody (green) and propidium iodide (staining the nuclei red). (*A*) In control neurons, 4G8 immunolabeled cytoplasm and neuronal processes. (*B*) The apoptotic cell (arrow), recognizable by a small strongly stained nucleus, shows 4G8 immunolabeling concentrated in the condensed cytoplasm. Two "naked nuclei" are also seen, whereas the remaining neurons show different degrees of apoptotic modifications. (*C, D, F,* and *G*) Cells were double-stained with 4G8 antibody (*C* and *F*) and rhodamine-conjugated WGA (*D* and *G*). The two chromophores are shown separately with the same color scale. An higher-magnification view of cells shown in *C, D, F,* and *G* is, respectively, reported in *E* and *H*, where the two chromophores are superimposed in the same image with a green/red color scale. (*E*) In control neurons, 4G8 (green) and WGA Golgi (red) staining colocalize (yellow), whereas in three apoptotic neurons (*H*, arrows), the 4G8 signal appears to be mostly condensed in cytoplasm and does not colocalize with the Golgi apparatus, which is fragmented.

creased Aβ production. The cytoplasmic condensation of Aβ reactivity, associated with the dispersal of Golgi apparatus, which we observed by immunocytochemistry, further supports the hypothesis of a deranged trafficking of Golgi-derived vesicles (containing APP C-terminal fragments) in the course of apoptosis. Altered vesicle sorting could be caused by the breakdown of microtubules that occurs in this apoptotic model as preliminary data indicate (unpublished results). The condensation of Golgi-derived protein vesicles is probably strictly related with the mechanism underlying the increase of APP products derived from β-secretase cleavage. Protease activation, as part of the apoptotic process in cerebellar granule cells, is known to occur (29). It is however unlikely that only β-secretase, but not the α-secretase, is selectively activated in

this event. The more likely explanation is that, after disruption of protein trafficking, APP metabolites are kept in an intracellular compartment in which a prolonged and preferential exposure to the β-secretase occurs. Cerebellar granule cells undergoing apoptosis have remarkable similarities to cultured cells expressing mutated PSs (28). In both models, an increased oligomerization of secreted soluble Aβ occurs, without changes in full-length APP production (28). Although the intracellular distribution of Aβ reactivity in cells expressing mutant PS has not been reported, PS mutations are likely to impair protein trafficking in the Golgi, as has been observed in *Caenorhabditis elegans* carrying mutations of spe-4, a PS analogue (30, 31). It has been reported that mutant PS2 induces apoptosis (3). Herein we show that neuronal apoptosis

is associated with an increase of amyloidogenic metabolism, indicating that different causes may, therefore, lead to a common neuronal disorder. This hypothesis has to be confirmed by analyzing APP metabolism in models of neuronal apoptosis mediated by different triggers such as growth factor deprivation, energetic metabolism default, and drug-induced cell cycle derangement. Another issue that needs to be clarified is whether the changes of APP processing that we observed are directly involved in the process of neuronal death, as suggested by the finding of the proapoptotic effect of mutant APP[717] (32). Several studies have provided evidence for the occurrence of DNA fragmentation from AD brains (5). Neuronal apoptosis has been so far interpreted as the consequence of the toxicity of extracellular Aβ aggregates, according to the amyloid "cascade" hypothesis. Our findings and those from experiments with mutant PS and APP[717] cells provide biological evidence that in AD, the Aβ overproduction can be the result of a primary neuronal degeneration, although, as suggested by the "cascade" hypothesis, it may also be the cause of further neuronal damage. The increased Aβ secretion may then activate a toxic loop that further accelerates the process of neurodegeneration. Moreover, the reduced proportion of secreted α-APP$_s$, which acts as a neurotrophic factor (33), can contribute to neuronal damage.

1. Selkoe, D. J. (1996) *J. Biol. Chem.* **271,** 1825–1828.
2. Roses, A. D. (1994) *J. Neuropathol. Exp. Neurol.* **53,** 429–437.
3. Wolozin, B., Iwasaky, K., Vito, P., Ganjei, J. K., Lacanà, E., Sunderland, T., Zhao, B., Kusiak, J. W., Wasco, W. & D'Adamio, L. (1996) *Science* **274,** 1710–1713.
4. Scheuner, D., Eckman, C., Jensen, M., Song, X., Citron, M., Suzuki, N., Bird, T. D., Hardy, J., Hutton, M., Kukull, W., Larson, E., Levy-Lahad, E., Viitanen, M., Peskind, E., Poorkaj, P., Schellenberg, G., Tanzi, R., Wasco, W., Lannfelt, L., Selkoe, D. & Younkin, S. (1996) *Nat. Med.* **2,** 864–870.
5. Su, J. H., Anderson, A. J., Cummings, B. J. & Cotman, C. W. (1994) *Neuroreport* **5,** 2529–2533.
6. D'Mello, S. R., Galli, C., Ciotti, M. T. & Calissano, P. (1993) *Proc. Natl. Acad. Sci. USA* **90,** 10989–10993.
7. Miller, M. T. & Johnson, E. M., Jr. (1996) *J. Neurosci.* **16,** 7487–7495.
8. Galli, C., Meucci, O., Scorziello, A., Werge, T. M., Calissano, P. & Schettini, G. (1995) *J. Neurosci.* **15,** 1172–1179.
9. Graham, M. E. & Burgoyne, R. D. (1993) *Eur. J. Neurosci.* **5,** 575–583.
10. Gallo, V., Ciotti, M. T., Coletti, A., Aloisi, F. & Levi, G. (1982) *Proc. Natl. Acad. Sci. USA* **79,** 7919–7923.
11. Trani, E., Ciotti, M. T., Rinaldi, A. M., Canu, N., Ferri, G. L., Levi, A. & Possenti, R. (1995) *J. Neurochem.* **65,** 2441–2449.
12. Levi, G., Aloisi, F., Ciotti, M. T. & Gallo, V. (1984) *Brain Res.* **290,** 77–86.
13. Mercanti, D., Galli, C., Liguori, M., Ciotti, M. T., Gullà, P. & Calissano, P. (1992) *Eur. J. Neurosci.* **4,** 733–744.
14. Busciglio, J., Gabuzda, D. H., Matsudaira, P. & Yankner, B. A. (1993) *Proc. Natl. Acad. Sci. USA* **90,** 2092–2096.
15. Teller, J. K., Russo, C., DeBusk, L. M., Angelini, G., Zaccheo, D., Dagna-Bricarelli, F., Scartezzini, P., Bertolini, S., Mann, D. M. A., Tabaton, M. & Gambetti, P. (1996) *Nat. Med.* **2,** 93–95.
16. Russo, C., Saido, T. C., DeBusk, L. M., Tabaton, M., Gambetti, P. & Teller, J. K. (1997) *FEBS Lett.* **409,** 411–416.
17. Kim, K. S., Miller, D. L., Sapienza, V. J., Chen, C.-M. J., Bai, C., Grundke-Iqbal, I., Currie, J. R. & Wisniewsky, H. M. (1988) *Neurosci. Res. Commun.* **2,** 121.
18. Podlisny, M. B., Tolan, D. R. & Selkoe, D. J. (1991) *Am. J. Pathol.* **138,** 1423–1435.
19. Podlisny, M. B., Ostaszewski, B. L., Squazzo, S. L., Koo, E. H., Rydell, R. E., Teplow, D. B. & Selkoe, D. J. (1995) *J. Biol. Chem.* **270,** 9564–9570.
20. Bush, A. I., Pettingell, W. H., Jr., de Paradis, M., Tanzi, R. E. & Wasco, W. (1994) *J. Biol. Chem.* **269,** 26618–26621.
21. Wasco, W., Gurubhagavatula, S., Paradis, M., Romano, D. M., Sisodia, S., Hyman, B. T., Neve, R. L. & Tanzi, R. (1993) *Nat. Genet.* **5,** 95–100.
22. Sprecher, C. A., Grant, F. J., Grimm, G., O'Hara, P. J., Norris, F., Norris, K. & Foster, D. C. (1993) *Biochemistry* **32,** 4481–4486.
23. Slunt, H. H., Thinakaran, G., Von Koch, C., Lo, A. C. Y., Tanzi, R. E. & Sisodia, S. S. (1994) *J. Biol. Chem.* **269,** 2637–2644.
24. Haass, C., Schlossmacher, M. G., Hung, A. Y., Vigo-Pelfrey, C., Mellon, A., Ostaszewski, B. L., Lieberburg, I., Koo, E. H., Schenk, D., Teplow, D. B. & Selkoe, D. J. (1992) *Nature (London)* **359,** 322–325.
25. Haass, C., Lemere, C. A., Capell, A., Citron, M., Seubert, P., Schenk, D., Lannfelt, L. & Selkoe, D. J. (1995) *Nat. Med.* **1,** 1291–1296.
26. Philpott, K. L., McCarthy, M. J., Becker, D., Gatchalian, C. & Rubin, L. L. (1996) *Eur. J. Neurosci.* **8,** 1906–1915.
27. Naidu, A., Quon, D. & Cordell, B. (1995) *J. Biol. Chem.* **270,** 1369–1374.
28. Xia, W., Zhang, J., Kholodenko, D., Citron, M., Podlisny, M. B., Teplow, D. B., Haass, C., Seubert, P., Koo, E. H. & Selkoe, D. J. (1997) *J. Biol. Chem.* **272,** 7977–7982.
29. Schulz, J. B., Weller, M. & Klockgether, T. (1996) *J. Neurosci.* **16,** 4696–4706.
30. Hardy, J. (1997) *Trends Neurosci.* **20,** 154–159.
31. L'Hernault, S. W. & Arduengo, P. M. (1992) *J. Cell Biol.* **119,** 55–68.
32. Yamatsuji, T., Matsui, T., Okamoto, T., Komatsuzaki, K., Takeda, S., Fukumoto, H., Iwatsubo, T., Suzuki, N., Asami-Okada, A., Ireland, S., Kinane, T. B., Giambarella, U. & Nishimoto, I. (1996) *Science* **272,** 1349–1352.
33. Furukawa, K., Sopher, B. L., Rydell, R. E., Begley, J. G., Pham, D. G., Martin, G. M., Fox, M. & Mattson, M. P. (1996) *J. Neurochem.* **67,** 1882–1896.